Japanese Journal of Gastroenterology and Hepatology

Review Article

ISSN: 2435-1210 | Volume 10

MRI Feature of Fontan Associated Liver Disease and Hepatocellular Carcinoma

Michinobu Nagao[1*] and Tomomi Kogiso[2]

[1]Department of Diagnostic Imaging and Nuclear Medicine, Tokyo Women's Medical University, 8-1 Kawada-cho, Shinjuku-ku, 162-8666, Tokyo, Japan

[2]Department of Gastroenterology, Tokyo Women's Medical University, 8-1 Kawada-cho, Shinjuku-ku, 162-8666, Tokyo, Japan

***Corresponding author:**

Michinobu Nagao, MD, PhD,
Department of Diagnostic Imaging and Nuclear Medicine, Tokyo Women's Medical University8-1 Kawada-cho, Shinjuku-ku, Tokyo 162-8666, Japan

Received: 02 Jan 2025
Accepted: 23 Jan 2025
Published: 29 Jan 2025
J Short Name: JJGH

Keywords:

Fontan-Associated Liver Disease; Hepatocellular Carcinoma; Magnetic Resonance Imaging; Gadolinium-Ethoxybenzyl-Diethylene-Triamine-Pentaacetic Acid

Citation:

Michinobu Nagao. MRI Feature of Fontan Associated Liver Disease and Hepatocellular Carcinoma.
J Gastro Hepato. 2025; V10(14): 1-9

1. Abstract

Gadolinium-ethoxybenzyl-diethylene-triamine-pentaacetic acid (Gd-EOB-DTPA) MRI has the advantage of simultaneously screening for hepatocellular carcinoma (HCC) and evaluating liver damage due to Fontan associated liver disease (FALD), and is suitable for follow-up of young patients because of the lack of X-ray exposure. In the Gd-EOB-DTPA hepatocyte phase, reticular low intensity mainly in the peripheral regions of the liver and decreased signal ratio of liver to spleen are characteristic findings reflecting FALD pathologies. HCC on FALD often shows high signal in the hepatocyte phase with no washout in the venous phase and no significant contrast effect in the arterial phase. FALD-occurring HCCs have a tendency toward slow enlargement, the development of partial low-signal areas in the hepatocyte phase, and diffusion restriction, which distinguish them from focal nodular hyperplasia (FNH)-like lesions. Recently, MR lymphangiography to noninvasively delineate lymphatic congestion occurring in FALD and cardiac MRI to analyze hepatic T1 map and hepatic strain for the assessment of liver fibrosis have been reported. This review focuses on the features of FALD and HCC on Gd-EOB-DTPA MRI and discusses upcoming MRI imaging and analytic technology, and introduces their clinical applications.

2. Introduction

Fontan procedure is performed for functional single ventricle hemodynamics such as tricuspid atresia, single ventricle syndrome, hypoplastic left ventricle syndrome, etc. Although the results of Fontan surgery have been improving, it is known that arrhythmia, cyanosis, thromboembolism, protein loosing gastroenteropathy, heart failure, pulmonary hypertension, liver cirrhosis, renal failure, and other systemic organ failure may occur over the long-term course. In particular, liver complications are called Fontan-associated liver disease (FALD), which not infrequently progresses to cirrhosis and hepatocellular carcinoma, and is reported to be associated with high mortality [1,2]. Of the 2,700 postoperative Fontan patients in Japan, 31 were diagnosed with cirrhosis or hepatocellular carcinoma (1.2%) and 5 died of liver disease (mortality rate 0.2%). The average age at diagnosis of cirrhosis and hepatocellular carcinoma (HCC) was 23 and 31 years young [3-5]. However, liver biopsies are often difficult to perform due to oral anticoagulant and thrombotic medications, low cardiac function, and concomitant malformations, making the diagnosis of cirrhosis difficult. Unlike other chronic liver diseases, FALD is a non-inflammatory liver fibrosis, so common liver function tests such as transaminases often do not show abnormalities [6]. Fibrosis markers such as type IV collagen, hyaluronic acid, and procollagen-III-peptide (P-III-P) are often elevated in FALD, but it is difficult to distinguish cirrhosis from non-cirrhosis [7]. Thus, blood biochemical tests are currently inconclusive, and imaging tests such as CT and MRI should be actively incorporated to screen for FALD and hepatocellular carcinoma. MRI does not have the X-ray exposure of CT and is easy to repeat in FALD patients, many of whom are young. Furthermore, MRI has a higher contrast resolution of lesions than CT and can produce different images for comprehensive tissue characterization. We review the evaluation of HCC on FALD with a focus on the topic of MRI.

3. Gd-EOB-DTPA MRI

Gadolinium-ethoxybenzyl-diethylene-triamine-pentaacetic acid (Gd-EOB-DTPA), a liver-specific contrast agent, can be used to evaluate the contrast effect on T1-weighted images as with conventional extracellular fluid contrast agents, and dynamic studies can be performed to image the hemodynamics of liver tumors. It has the advantage of visualizing differences in hepatocyte function from the hepatocyte phase taken up by hepatocytes at 15 minutes after administration. Hepatocyte uptake is mediated by the hepatocyte membrane transporter organic anion transporter polypeptides (OATP)1B3/OATP1B1, which is expressed on the sinusoidal side [8]. The imaging protocol for Gd-EOB-DTPA takes about 20 minutes in total, which is longer than contrast-enhanced CT (Figure 1). However, it is of great clinical significance to simultaneously screen for HCC and evaluate the degree of liver damage by blood flow and function information in a single examination in FALD treatment.

4. Features of FALD

After Fontan surgery, chronic elevated central venous pressure results in hepatic venous stasis and dilation of the sinusoids around the central veins. Edema and hepatic ischemia around the sinusoids progress to fibrosis without inflammation in the portal area1). In the EOB hepatocyte phase, reticular hypoperfusion mainly in the peripheral regions of the liver is a characteristic finding reflecting these pathologies (Figure 2) [9]. Diffuse signal reduction in the liver parenchyma in the EOB hepatocyte phase is used as an indicator of fibrosis, such as the hepatosplenic signal ratio, which can be easily calculated [10]. In FALD, some patients rapidly progress to compensated cirrhosis within a few years (Figure 3).

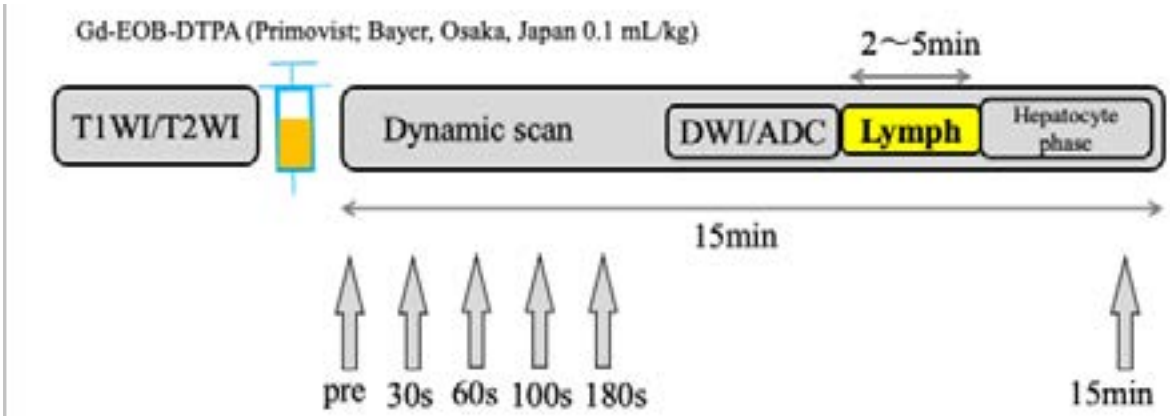

Figure 1: Gd-EOB-DTPA MRI with 3.0-Teslar scanner (Ingenia CX, 3.0-T, Philips Healthcare) protocol for FALD evaluation. T1WI: T1-weighted image, T2WI: T2-weighted image, DWI: Diffusion weighted image, ADC: apparent diffusion coefficient, Lymph: lymphangiography.

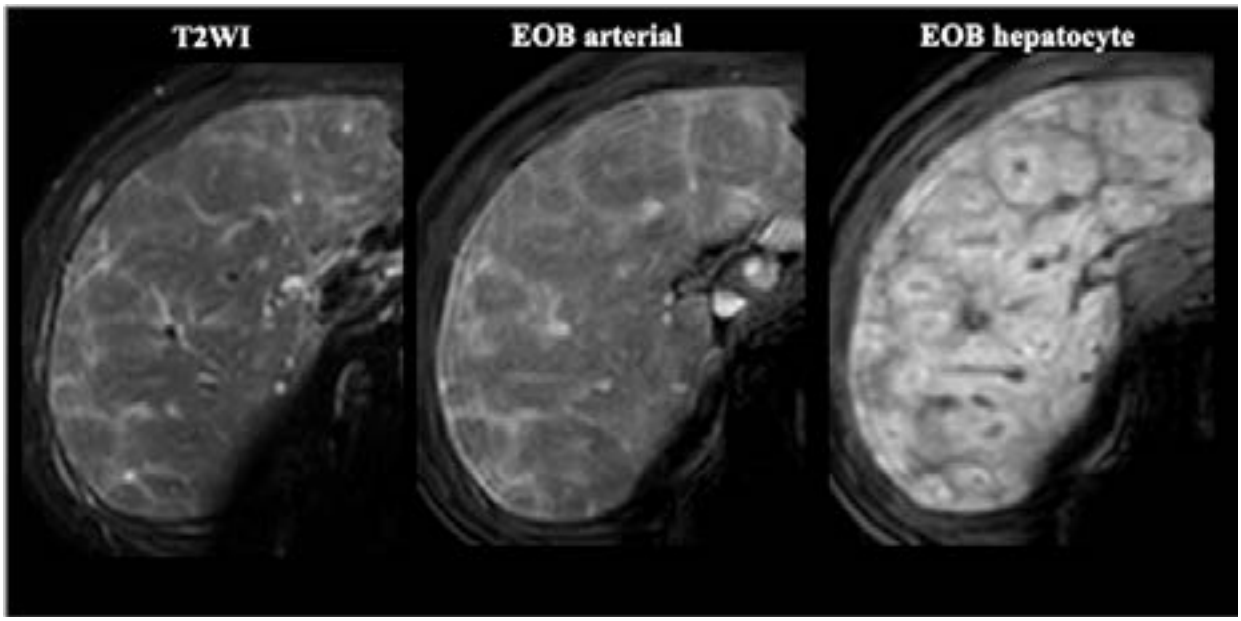

Figure 2: Woman in her 20s. Eight years after total cava-pulmonary connection for congenital single ventricle. T2-weighted image (left), Gd-EOB-DTPA contrast-enhanced dynamic MRI 30 seconds after contrast injection (center), hepatocyte phase (right). T2-weighted high-signal areas are seen mainly in the subcapsule to the periphery of the liver, in line with the hepatic vein and portal vein. The contrast-enhanced dynamic early staining area coincides with the low-signal area of the hepatocyte phase. The reticular low-signal areas in the hepatocyte phase are characteristic of FALD, with a so-called "reverse lobulation" distribution of the hepatic lobules.

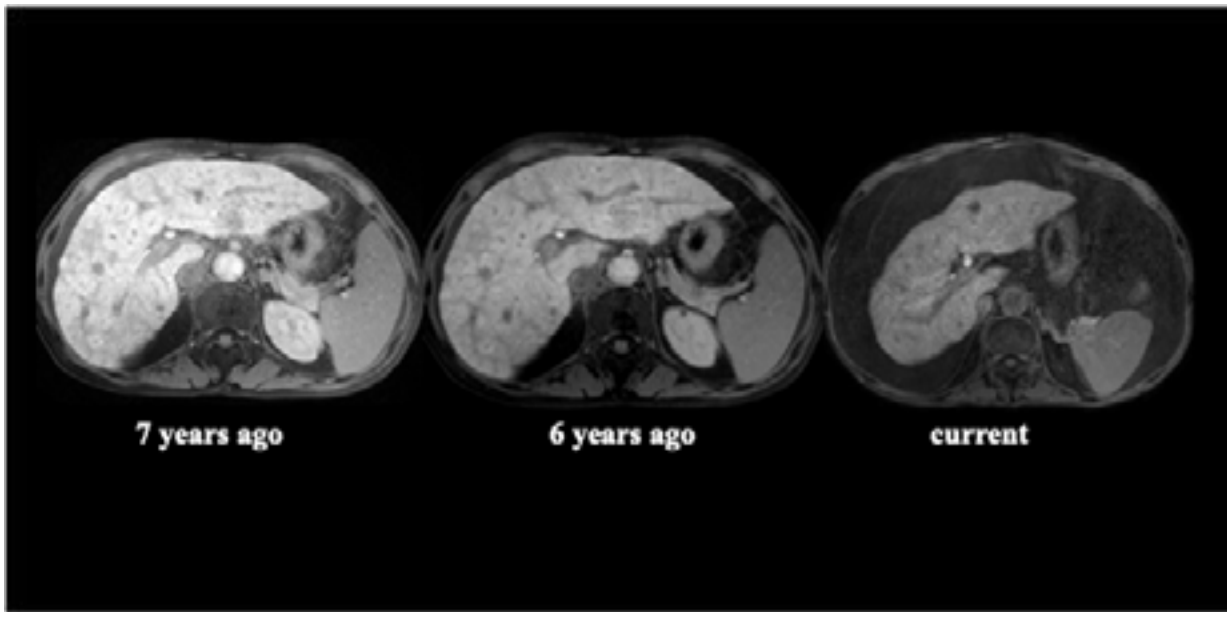

Figure 3: Woman in her 40s, Fontan procedure performed 25 years ago for congenital single ventricle. The course of the Gd-EOB-DTPA hepatocyte phase shows marked atrophy of the liver compared to 6-7 years ago. The signal ratio of the liver to spleen decreased from 1.21 seven years ago, 1.12 six years ago, to 1.06 now, suggesting progressive fibrosis.

5. Differential Diagnosis between HCC and FNH-Like Lesion

In the sinusoids, in addition to thrombus formation and ischemia, fibrosis is accelerated by decreased oxygen supply to hepatocytes, leading to progression to cirrhosis. In normal liver, the ratio of portal to hepatic arterial blood flow is approximately 3:1, but the decrease in portal blood flow associated with fibrosis induces a compensatory increase in hepatic arterial blood flow, which is called hepatic arterial buffer response (HABR). It has been reported that liver tumors without HCC occur in about 10% of Fontan patients11). The majority of nodules are focal nodular hyperplasia (FNH) or FNH-like lesions, which are less than 2 cm in length and multiple in number1, [10]. In HCC with FALD, early contrast enhancement on EOB-MRI is mild to moderate, and no washout of the contrast delayed phase is seen. The early contrast effect is stronger for FNH-like lesions than for HCC. FALD-derived HCCs often show high signal in the hepatocyte phase with mild early contrast effect on EOB-MRI (Figure 4) [10,12]. These suggest low portal vein infiltration and increased expression of the hepatocyte membrane transporter OATP1B3, suggesting a low biological grade. A low signal in the hepatocyte phase is a decisive factor for HCC, Fontan-occurring HCC is characterized by partial low signal within the high-signal mass and an increase over time in the low-signal area (Figure 4). This finding can be differentiated from FNH like lesions, which show a homogeneous high-signal area (Figure 5). Diffusion-weighted imaging shows diffusion restriction, which is a reason to suspect HCC; however, subcapsular nodules under the hepatic capsule require caution due to motion and magnetic susceptibility change artifacts (Figure 6). If hypervascularized nodules larger than 2 cm in diameter are present, it is important to closely monitor the change in size and intra-mass properties. Some FNH-like lesions occasionally regress spontaneously (Figure 7). Table 1 summarizes the characteristics of MRI findings of HCC and FNH-like lesion.Hepatic dynamic CT is essential for the diagnosis of HCC and the determination of therapeutic efficacy, and four phases are performed: simple, arterial phase, portal venous phase, and equilibrium phase. Repeated liver dynamic CT may increase radiation exposure. In addition, although CT has superior spatial resolution, contrast resolution of lesions is inferior to MRI.

6. MR Lymphagiography

Increased central venous pressure and decreased cardiac output in the Fontan circulation can cause permanent lymphatic congestion, refractory ascites, and protein-leakage gastropathy. Anatomical information on abnormal lymphatic channels is necessary to identify lymphatic leaks during percutaneous lymphatic embolization [13]. However, direct puncture of the lymphatic vessels carries a high risk of bleeding and has a low success rate, so it is difficult to identify lymphatic leaks before treatment. Safe and reproducible noninvasive lymphangiography is needed. MR lymphangiography with a 3D-turbo spin echo with dual inversion recover tissue-specific image contrast optimization using dual-TI to suppress fat and blood signals, demonstrates the localization and extent of theabnormal lymphatic pathways in Fontan circulation (Figure 8) [14-15].Minimally invasive MR lymphangiography has promise as an aid in FALD treatment strategies.

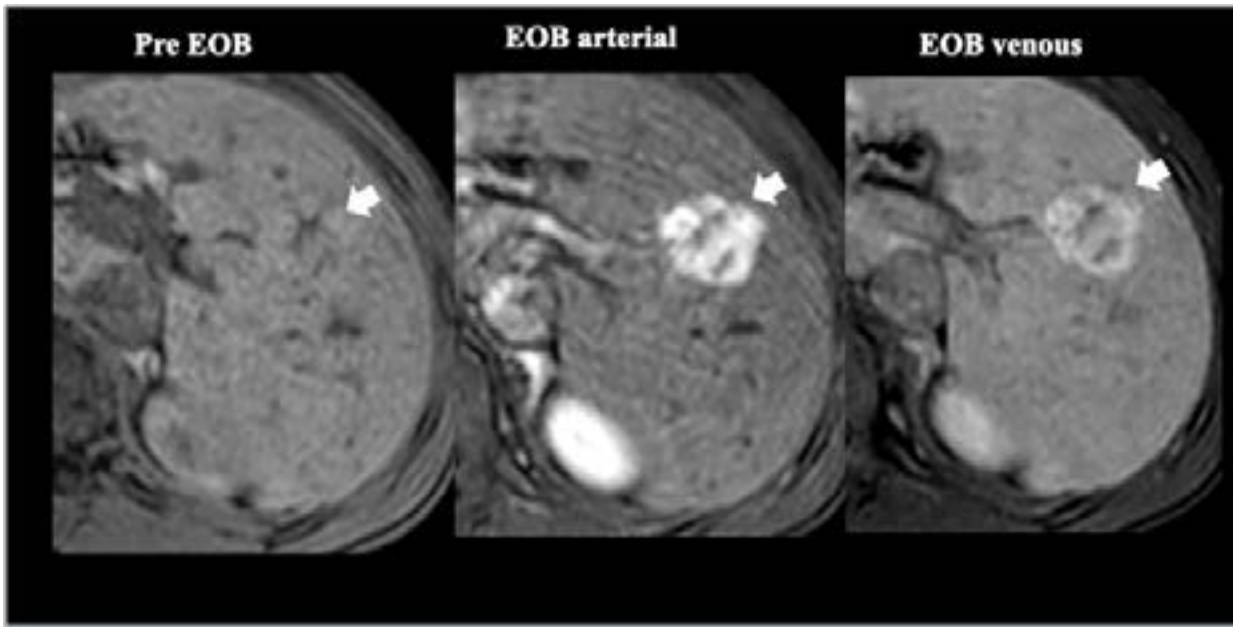

Figure 4: Male in his 20s. 15 years after total cava-pulmonary connection for congenital single ventricle and heterotaxysyndrome. Liver biopsy revealed hepatocellular carcinoma, and proton beam therapy was performed.
A: Gd-EOB-DTPA contrast dynamic MRI before contrast (left), 30 sec after contrast (center), 180 sec after contrast (right) showing a lobulated, internally heterogeneous, early-staining mass of approximately 3cm in the diameter (arrow). No washout is seen in the late contrast phase.

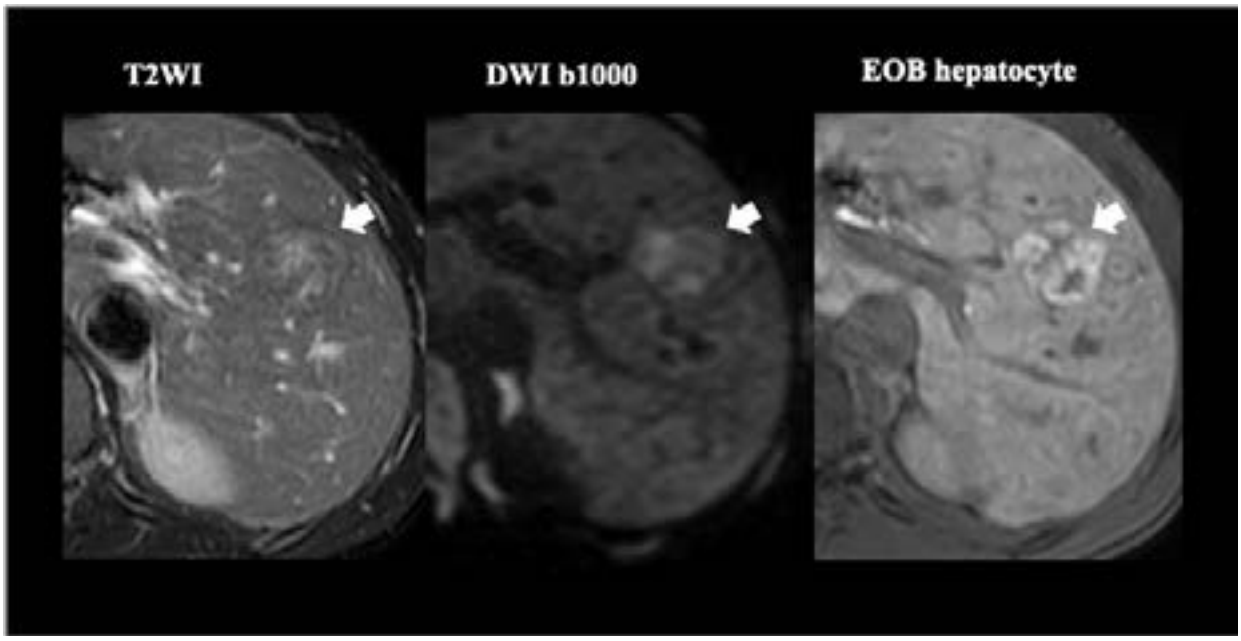

Figure 4B: Fat-suppressed T2-weighted image (left) shows pale high signal in the interior and low signal cover at the margins (arrow). Diffusion-weighted image (b-1000, center) shows mild diffusion restriction (arrow); EOB hepatocyte phase (right) shows mosaic-like low to high signal (arrow).

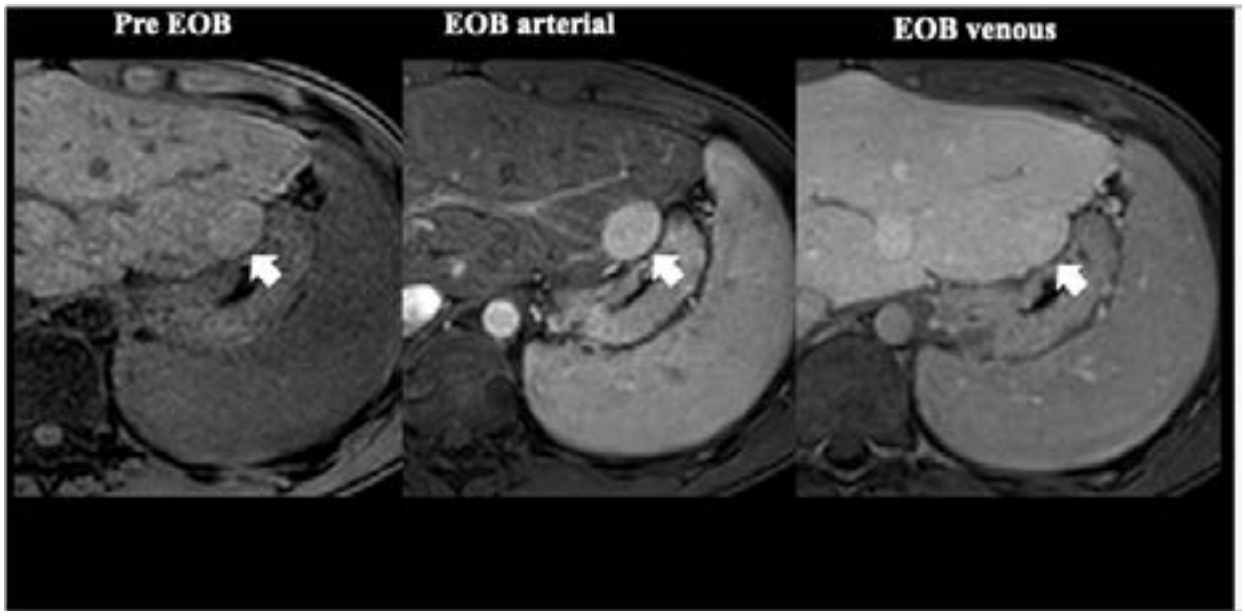

Figure 5: Male in his 20s. After 13 years of total cava-pulmonary connection for congenital single ventricle, focal nodular hyperplasia like lesion (FNH-like lesion) in the liver that has not changed for 3 years.
A: Gd-EOB-DTPA contrast dynamic MRI before contrast (left), 30 sec after contrast (center), 180 sec after contrast (right). A nodule with a diameter of approximately 2 cm is seen under the capsule in the left lobe of the liver, with smooth margins and homogeneous staining early in contrast (arrow). The signal is comparable to that of the surrounding liver parenchyma in the late contrast phase (arrows).

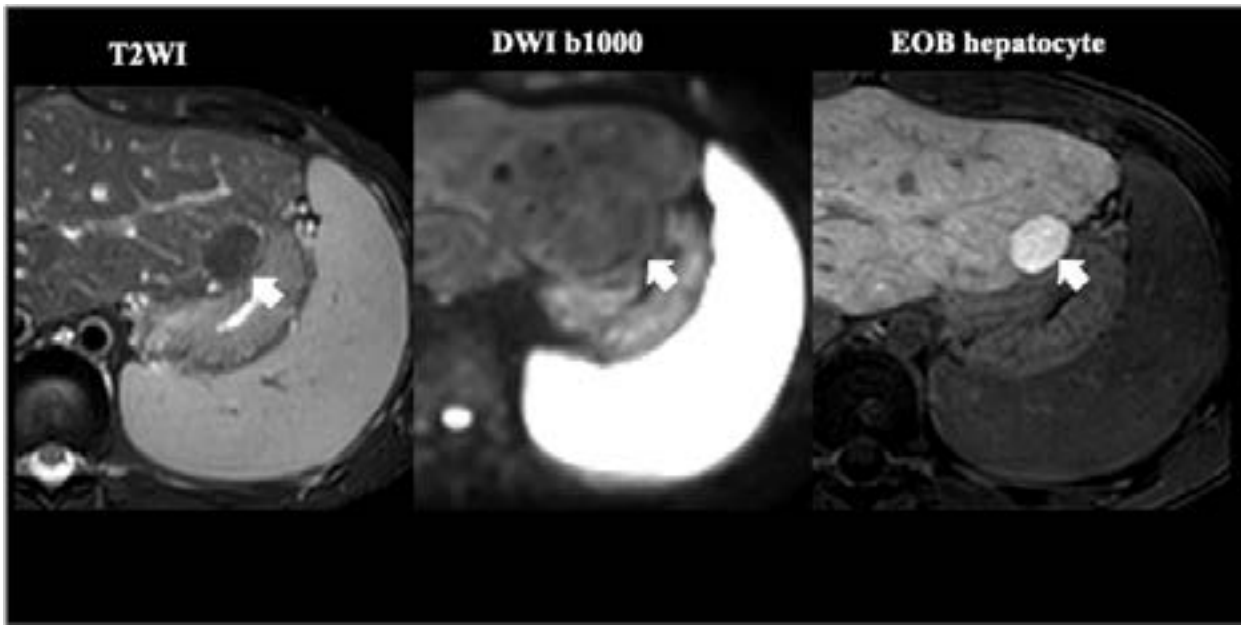

Figure 5 B: Fat-suppressed T2-weighted image (left) shows mildly lower signal than surrounding liver (arrow); diffusion-weighted image (b-1000, center) shows no diffusion restriction; EOB hepatocyte phase shows homogeneous high signal in the nodules (arrow).

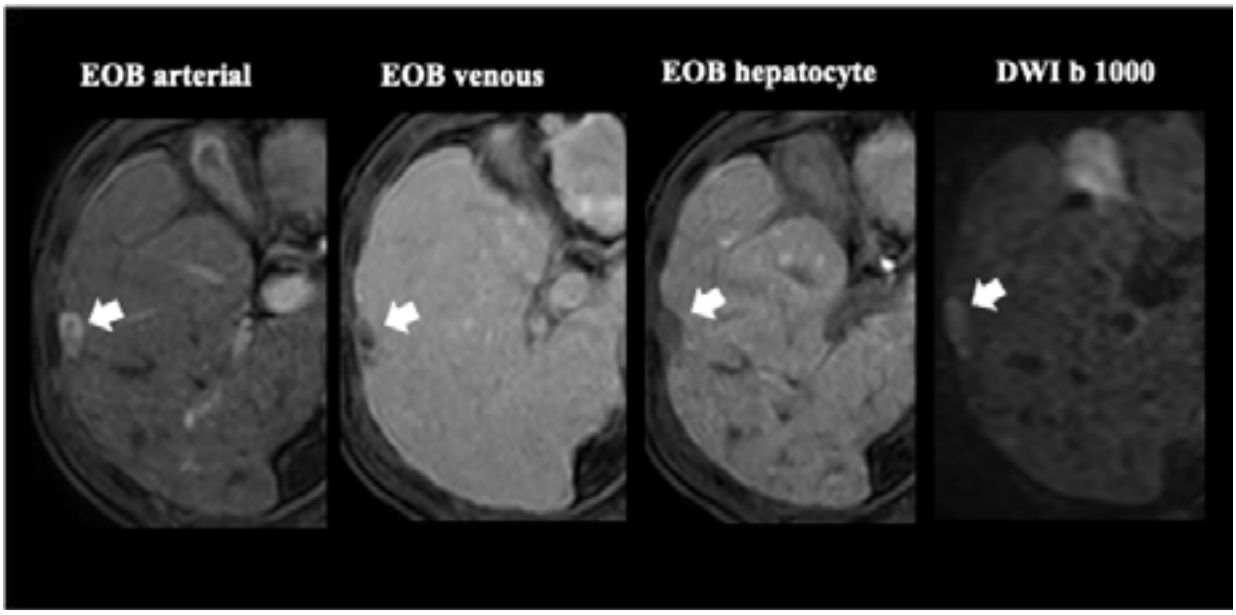

Figure 6: A woman in her 30s. Gd-EOB-DTPAMRI performed due to elevated alpha-fetoprotein shows a ring-shaped nodule with a diameter of less than 2 cm under the capsule of the right lobe in early contrast (left, arrow). Diffusion-weighted images (b-1000, center) show mild diffusion restriction and low signal in the hepatocyte phase (right, arrow). The tumor was resected and pathologically diagnosed as HCC.

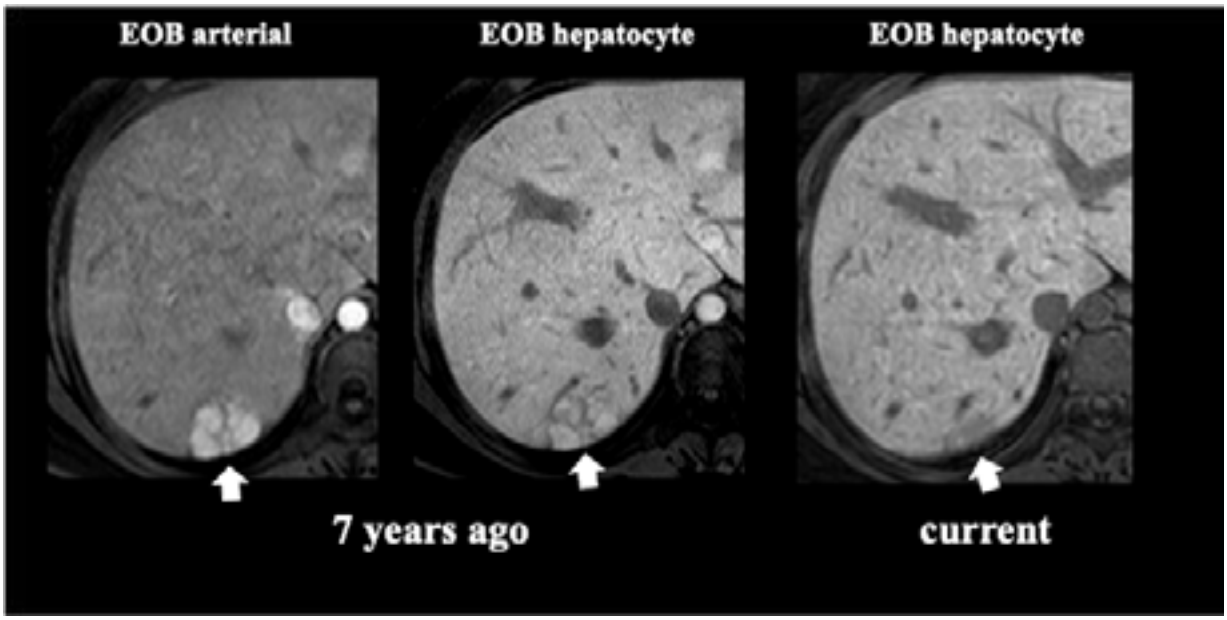

Figure 7: Female in her 20's. 15 years after total cava-pulmonary connection for congenital single ventricle. The mass is uniformly stained at 30 seconds (left) after Gd-EOB-DTPA contrast of about 2.5cm in diameter under the capsule of the right lobe of the liver, and pale high signal is seen in the hepatocyte phase (center, arrow). 7 years later in the hepatocyte phase of Gd-EOB-DTPA (right), the mass has disappeared and is considered to be a spontaneous regression of FNH-like lesion.

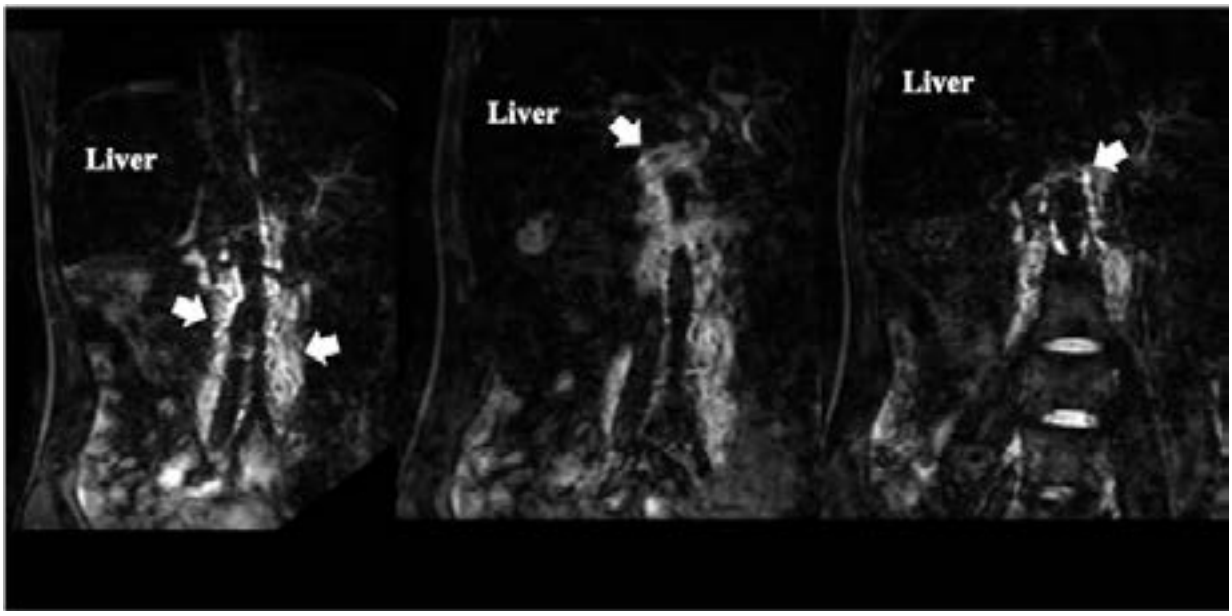

Figure 8: A man in his late teens who underwent Fontan procedure 15 years ago for congenital single ventricle disease. MR lymphangiography demonstrates high signal lymphatic congestion peri-lumber vertebra (left, arrow) and peri-bile duct to peri-duodenum (center, arrow), and lower thoracic duct (right, arrow).

7. Cardiac MRI Applications

Cardiac MRI is essential for the assessment of single ventricle function and hemodynamics in the Fontan circulation. Myocardial T1 mapping on cardiac MRI is standardized as a quantitative assessment of myocardial edema and fibrosis. Myocardial T1 mapping can simultaneously measure T1 values in the upper portion of the liver, and prolonged hepatic T1 values are observed in patients with FALD compared to other complex cardiac malformations (Figure 9) [16]. This result corroborates liver edema and fibrosis in FALD. Cardiac cine MRI can also calculate the hepatic strain, which is the passive deformation of the liver in contact with the subepicardial surface due to cardiac pulsation, and it has been reported that patients with FALD have a reduced hepatic strain compared to other complex cardiac malformations [17]. Fontan procedure can be divided into the initial atrio-pulmonary connection, the subsequent lateral tunnel, and the total cavopulmonary connection. In APC-Fontan, upstream right atrial stasis leads to a congested liver and is associated with the development of FALD (Figure 10) [18]. Cardiac MRI should be effectively utilized for comprehensive evaluation of FALD, which is a cardiohepatic interconnected disease.

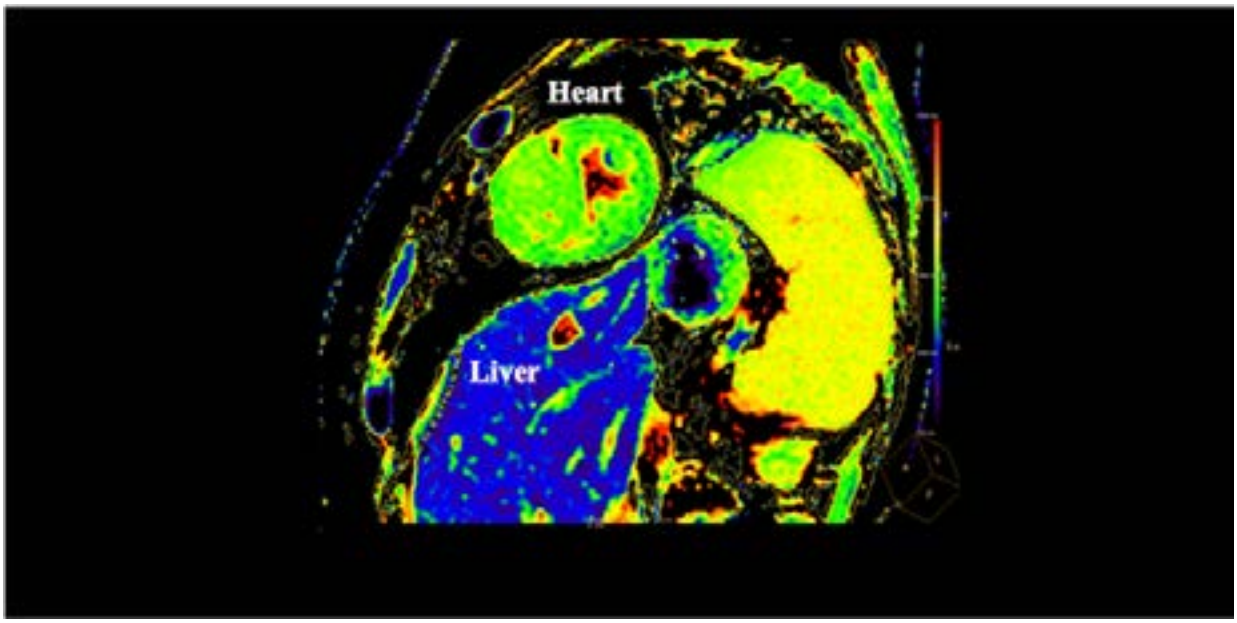

Figure 9: Myocardial T1 mapping scanned with the MOLII method and 3 tesla scanner for postoperative Fontan patient. Native T1 values for the liver are shorter than for the myocardium, and the liver is shown in blue. Liver T1 values prolonged in controls, averaging 770 msec vs. 960 msec in post-Fontan patients, suggesting edema and fibrosis in the liver.

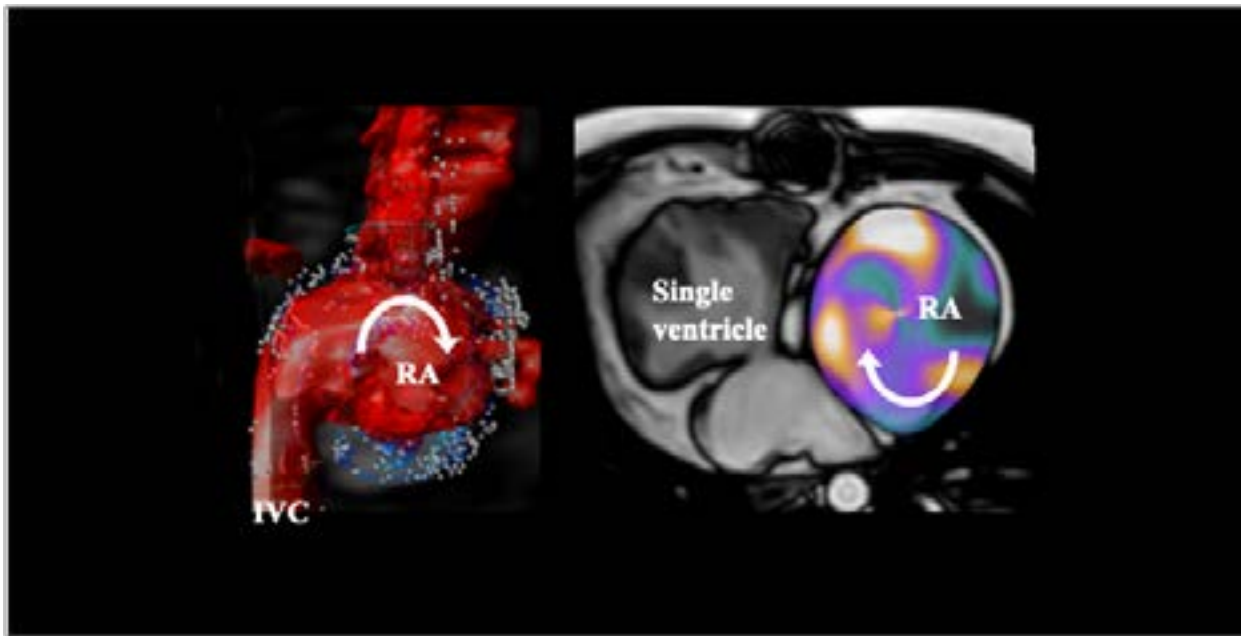

Figure 10: Male in his 20s, 15 years after APC-Fontan procedure for congenital biventricular single ventricle. 4D flow MRI (left) shows arcuate blood flow particles from cephalad to caudal in the dilating right atrium, forming a slow vortex flow (arrow). Vortex flow map using cine MRI and voxel tracking (right) shows clockwise rotating vortex flow in hot color (arrow) in the expanding right atrium. Vortical flow is the driving force in the Fontan circulation, and it prevents congestion of the inferior vena cava and hepatic congestion. Upstream circulatory assessment is important in the development of FALD. RA: right atrium.

8. Summary

Gd-EOB-DTPA MRI can characterize the FALD pathology and FALD-onset HCC as distinct from other liver diseases; Gd-EOB-DTPA MRI is a minimally invasive and effective tool for screening HCC and evaluating fibrosis in FALD patients because of the lack of x-ray exposure. In addition, it is expected that the advanced technologies of cardiac MRI and MRI hemodynamic analysis will be utilized to elucidate the new pathophysiology of FALD. In the future, more Fontan patients will benefit from the expansion of MRI indications for cardiac electrical devices with the development of wide-band MRI [19].

9. Acknowledgments:

This work was supported by the Japan Society for the Promotion of Science (JSPS) KAKENHI (grant no. 22K07806).

References

1. Kogiso T, Tokushige K. Fontan-associated liver disease and hepatocellular carcinoma in adults. Scientific Reports. 2020; 10: 21742.
2. Yoon JS, Lee DH, Cho EJ. Risk of liver cirrhosis and hepatocellular carcinoma after Fontan operation: a need for surveillance. Cancers. 2020; 12: 1805.
3. Nii M, Inuzuka R, Inai K. Incident and expected probability of liver cirrhosis and hepatocellular carcinoma after Fontan operation. Circulation. 2021; 144 (25): 2043-2045.
4. Kuwabara M, Niwa K, Toyoda T. Liver cirrhosis and/or hepatocellular carcinoma occurring late after the Fontan procedure: a nationwide survey in Japan. Circ J. 2018; 82: 1155-1160.
5. Ohfuji S, Tanaka A, Kogiso T, Kanto T. Epidemiology of Fontan-associated liver disease in Japan: Results from a nationwide survey in 2021. Hepato Res. 2024; 54(10): 931-940
6. Guha IN, Bokhandi S, Ahmad Z, Sheron N, Cope R, Marshall C. Structural and functional uncoupling of liver performance in the Fontan circulation. Int J Cardiol. 2011; 164: 77-81.
7. Kogiso T, Takayanagi K, Ishizuka T. Serum level of full-length connective tissue growth factor reflects liver fibrosis stage in patients with Fontan-associated liver disease. Plos One. 2024; 19(1): e0296375.
8. Kitao A, Zen Y, Matsui O. Hepatocellular carcinoma: signal intensity at gadoxetic acid-enhanced MR imaging-correlation with molecular transporters and histopathological features. Radiology. 2010; 256: 817-826.
9. Nakajima K, Seki M, Hatakeyama S. Visual liver assessment using Gd-EOB-DTPA enhanced magnetic resonance imaging of patients in the early post-Fontan period. Scientific Reports. 2020; 10: 4909.
10. Yamamoto A, Nagao M, Inoue A. Prediction of hepatocellular carcinoma in patients with Fontan-associated liver disease using gadolinium ethoxybenzyl diethylenetriamine pentaacetic acid magnetic resonance imaging. Hepato Res. 2024.
11. Kogiso T, Tokuhara D, Ohfuji S. Evaluation of diagnostic criteria for mild-to-advanced stages of Fontan-associated liver disease: A nationwide epidemiological survey in Japan. Hepato Res. 2024.
12. Shiina Y, Inai K, Sakai R. Hepatocellular carcinoma and focal nodular hyperplasia in patients with Fontan-associated liver disease: characterization using dynamic gadolinium ethoxybenzyl diethylenetriamine pentaacetic acid-enhanced MRI. Clin Radiol. 2022; 78(3): e197-e203.

13. Maleux G, Storme E, Cools B, Heying R, Boshoff D. Percutaneous embolization of lymphatic fistulae as treatment for protein-losing enteropathy and plasticbronchitis in patients with failing Fontan circulation. Catheter Cardiovasc Interv. 2019; 94(7): 996-1002.

14. Shiina Y, Inai K, Shimada E. Abdominal lymphatic pathway in Fontan circulation using non-invasive magnetic resonance lymphadenopathy. Heart and Vessels. 2023; 38(7): 581-587.

15. Yoneyama M, Ball M, Azuma M. Robust motion-compensated lumber spin bone imaging using 3D UTE with broadband inversion recovery pulse and k-space weighted navigator gating. Proc Intl Soc Mag Reson Med. 2019; 27: 0133.

16. Shiina Y, Inai K, Ohashi R, Nagao M. Potential of liver T1 mapping for the detection of Fontan-associated liver disease in adults. Magn Reson Med Sci. 2020; 20(3): 295-302.

17. Ohashi R, Nagao M, Ishizaki U. Liver strain using feature tracking of cine cardiac magnetic resonance imaging: assessment of liver dysfunction in patients with Fontan circulation and tetralogy of Fallot. Pediatri Cardiol. 2020; 41(19): 389-397.

18. Ishizaki U, Nagao M, Shiina Y. Prediction of Fontan-associated liver disease using a novel cine magnetic resonance imaging "vortex flow map" in the right atrium. Circ J 2018; 82(8): 2143-2151.

19. Patel HN, Wang S, Rao S. Impact of wideband cardiac magnetic resonance on diagnosis, decision-making and outcomes in patients with implantable cardioverter defibrillators. Eur Heart J Cardiovasc Imaging. 2023; 24: 181-189.